9.2 THE INFLUENCE OF TEMPORALLY-VARYING VERTICAL WIND SHEAR ON NUMERICALLY SIMULATED CONVECTIVE STORMS

Jaclyn Kost* and Yvette P. Richardson
Pennsylvania State University, University Park, PA

1. INTRODUCTION

The understanding of severe thunderstorm behavior has increased rapidly through direct measurements, improved theories, and numerical simulations. Specifically, it has been recognized using these methods that convective storm type is strongly influenced by the larger-scale environment. For example, previous numerical simulations have produced specific thunderstorm morphologies when using prescribed steady-state, horizontally homogeneous environments (e.g., Weisman and Klemp, 1982, 1984). Though indeed useful in advancing our knowledge, conceptual models derived from such investigations fall short when large-scale conditions change over a storm's lifetime. Consideration of such evolving environments within numerical simulations may provide a step toward further understanding of observed thunderstorm morphology and evolution.

In this study, we attempt to isolate the impact of temporally-varying environmental vertical wind shear upon modeled convection by altering speed and/or directional vertical shear in a horizontally-homogeneous manner over the lifetimes of simulated storms. This is similar to Richardson (1996) but includes a much more extensive suite of experiments. By conducting such idealized simulations in a horizontally homogeneous environment, changes in storm morphology, when compared to control simulations using a steady-state environment, can be attributed directly to the time-varying conditions. It is hoped that these results, when considered alongside those gained from idealized, spatially-inhomogeneous environment simulations (e.g., Richardson, 1999), will take us another step closer to understanding storm behavior in complex observed environments.

2. MODEL SPECIFICATIONS

The numerical model used in this investigation is version 4.5.2 of the Advanced Regional Prediction System (ARPS) (Xue et al., 1995). In this study, we use a three-category ice microphysics scheme, a flux-corrected transport scheme for advection of potential temperature perturbations and water variables, a 1.5-order turbulent kinetic energy (TKE) closure scheme (Moeng and Wyngaard, 1988), and a 4th order horizontal and 2nd order vertical advection scheme for momentum. The Coriolis force as well as surface physics and terrain are not used in these simulations.

**Corresponding Author Address*: Jaclyn Kost, Department of Meteorology, The Pennsylvania State University, University Park, PA 16802; e-mail: jkk136@psu.edu.

To accommodate time-varying environments, changes to the formulation of open lateral boundary conditions, zonal and meridional wind component calculations, the Asselin (1972) time filter, and domain translations are made. Details of these modifications can be found in Kost (2004). The horizontal grid spacing is 1.0 km, and the vertical grid spacing is 100 m up to 1.4 km with stretching applied between 1.4 km and 20 km. Storms are initiated with a 2 K warm thermal perturbation having a horizontal radius of 10 km and vertical radius of 1.4 km. The analytic sounding used is that of Weisman and Klemp (1982) with a surface mixing ratio of 15 g kg^{-1}. For straightline hodograph environments, symmetric conditions are prescribed at the northern domain boundary for computational efficiency.

3. RESULTS

Changes in large-scale vertical wind shear are achieved by specifying the initial and final environmental wind profiles desired and using these to prescribe accelerations at each vertical level. These accelerations are applied over the course of three hours starting at either the initiation time or, for comparison purposes, one hour after initiation, in which case the simulation is extended to four hours. It is felt that this time period for the shear variation is consistent with larger-scale features although perhaps toward the higher end of expected rates of change. Corresponding steady-state control runs are performed using the initial and final environmental hodographs of the respective temporally-varying simulations. Comparison between the experimental and control simulations allows one to isolate the influence of the temporally-varying environments.

3.1 *Weak-to-Strong Shear, Straightline Hodographs*

In these experiments, environmental wind profiles are defined by straightline hodographs according to $u=U_s\tanh(z/z_s)$, where z_s is 3000 m and U_s varies. As time progresses, the magnitude of the vertical wind shear increases from relatively weak (U_s=15 m s^{-1}) to strong (U_s=30 m s^{-1}). Given such conditions, a modeled storm could be expected to simply transition from a multicell to a supercell (as related to the results of Weisman and Klemp (1982) for the two shear regimes). As shown in Fig. 1, however, this is not what occurs. Whereas the midlevel storm structures of the weak-shear control case at 2.5 hours (Fig. 1a) are indicative of multicells (having transient updrafts that lack defining rotation) and those of the strong-shear control case (Fig. 1b) exhibit supercells (with relatively stronger, rotating updrafts), the experimental case (Fig. 1c) produces a

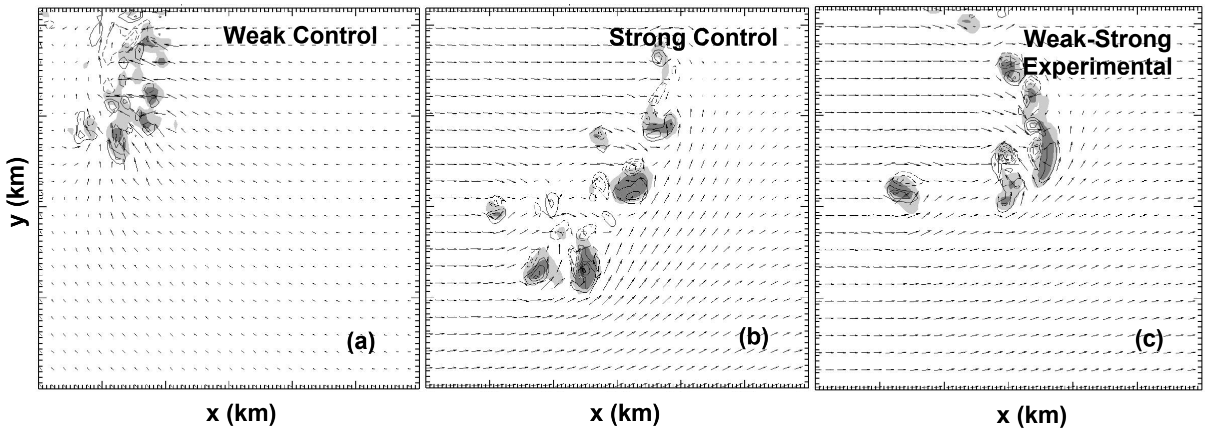

Figure 1: Horizontal cross-sections of vertical velocity (m s^{-1}, shaded), vertical vorticity (s^{-1}, contoured), and horizontal winds (m s^{-1}) at z = 4.6 km for straightline simulations in a 96 km x 67 km domain at 2.5 hr. Panels (a), (b), and (c) are for the weak control, strong control, and weak-to-strong experimental cases. Vertical velocity values greater than 15 m s^{-1} are darkly shaded. Vertical vorticity values are contoured every 5x10^{-3} s^{-1} (positive solid, negative dashed). Horizontal winds are plotted every 3 grid points with the unit vector representing 15 m s^{-1}. Tick marks are spaced at 1 km intervals. Symmetric conditions apply at the northern boundarv.

weakly-rotating, bow-like updraft structure in addition to an isolated, cyclonically rotating convective cell. From this midlevel perspective, it appears that a temporal increase in shear magnitude for a straightline hodograph environment serves to organize multicell storms along the leading edge of the system into bowed complexes. Similar results have been documented by Richardson (1999) for convection initiated in a multicellular-supportive environment and moving into a region of relatively stronger shear. We also note that this straightline hodograph environment characterized by a temporal increase in shear magnitude is supportive of isolated, rotating storms away from the main cluster of convective cells. Such isolated convection, however, appears to be a transient feature in the simulation.

Interesting results also are obtained when the change in shear magnitude is delayed such that it begins one hour after storm initiation. In this case, developing convection is embedded within a relatively weaker-shear environment for a longer time period compared with storms in the previous experiment. Comparison of midlevel features for these simulations illustrates that delaying the change in shear until after a significant cold pool has developed results in overall weaker storms that have a more difficult time transitioning into more organized forms of convection. The dynamics established early in the storm lifetime are not as easily overcome by the addition of increased environmental vertical shear.

3.2 Weak-to-Strong Shear, Curved Hodographs

In these experiments, we investigate the impact of increased vertical wind shear when the environmental wind profile follows a clockwise-curved hodograph. Again, we employ both weak and strong control cases with no temporal shear variation (corresponding to Weisman and Klemp (1984)). The radius of the half circle hodograph is 6.0 m s^{-1} for the weak case and 12.5 m s^{-1} for the strong case. Based on previous studies, we would conjecture that a temporal shear increase in such an environment could aid in transforming convection from overall multicellular to a mix of multicellular on the left flank and supercellular on the right-flank. As time progresses in the experimental simulation, left and right flank cells become distinct yet remain spatially close to one another. Midlevel right flank updrafts in this case appear as quasi-linear bands with weakly- associated rotation through 2.5 hours. This is unlike the weak-shear control case, which remains multicellular, or the strong-shear control case, which has a distinct, rotating right-flank storm. By the end of the 3 hour simulation (Fig. 2), the temporally-variable model run exhibits an isolated, right-flank cell with a strong updraft and net cyclonic rotation (Fig. 2c) that seems to have evolved from the quasi-linear band. At this time, the midlevel structure appears more similar to that of the strong-shear control case (Figure 2b) than the weak-shear control case (Figure 2a). Therefore, this shear change acts to transform convection from a purely multicellular complex into one containing a right flank supercell. As expected, an adjustment time to the stronger shear is necessary before achieving notable enhancement of right-flank storms.

To again study the effect of delaying the change in shear, we postpone the weak-to-strong shear transition in this clockwise-curved hodograph environment such that the change begins one hour after initiation. This delayed shear change produces a relatively weaker, short-lived initial right-flank cell. In this case, left- and right-flank activity does not become isolated, and, as shown in Fig. 3, any newly-developed right-flank activity is not sustained (Fig. 3b) compared with the earlier shear change case (Fig. 3a) at the end of the four hour

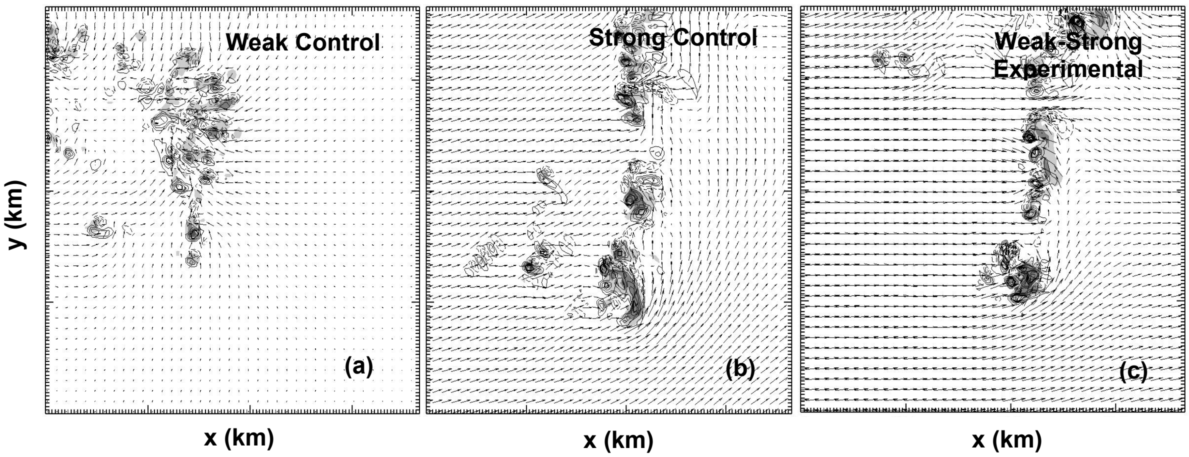

Figure 2: Horizontal cross-sections of vertical velocity (m s^{-1}, shaded), vertical vorticity (s^{-1}, contoured), and horizontal winds (m s^{-1}) at z = 4.6 km for curved simulations at 3 hours in a 117 km x 117 km domain. Panels (a), (b), and (c) are for weak control, strong control, and weak-to-strong experimental cases. Vertical velocity values greater than 15 m s^{-1} are darkly shaded. Vertical vorticity values are contoured every 5x10^{-3} s^{-1} (positive solid, negative dashed). Grid-relative horizontal winds are plotted every 3 grid points with the unit vector representing 11 m s^{-1}. Tick marks are spaced at 1 km intervals.

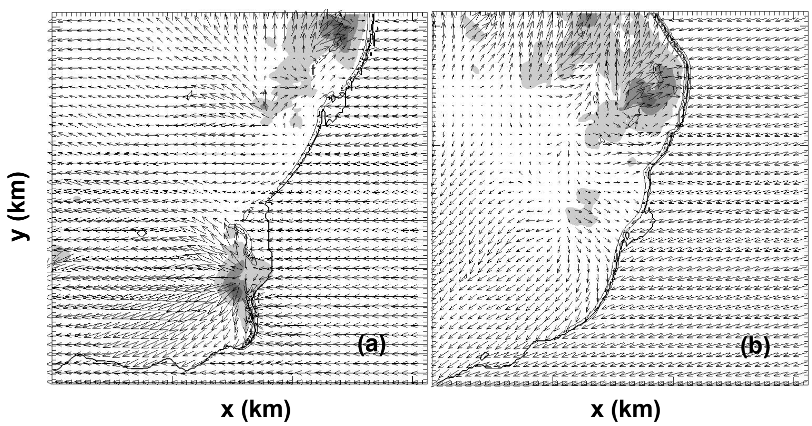

Figure 3: Low-level storm structure (0.10 km) for experimental curved hodograph simulations with a 117 km x 117 km domain. Panels (a), and (b) are at 4 hr for the early shear change and delayed shear change cases, respectively. Total water mixing ratio (g kg^{-1}) is darkly shaded for values greater than 4 g kg^{-1}, and the -1 K potential temperature perturbation contour is thickly drawn. Thin contours are positive vertical velocity (m s^{-1}). Grid-relative horizontal winds are spaced every 3 grid points with the unit vector representing 11 m s^{-1}. Tick marks are spaced at 1.5 km intervals.

simulation. Thus, simply delaying the increase in shear until after the cold pool has developed makes a difference in the development of a right-flank supercell.

3.3 Weak Shear, Straightline-to-Tail Hodographs

In these experiments, low-level clockwise hodograph curvature is added to an initially straightline hodograph over time in a weakly-sheared environment (U_s=15 m s^{-1}), resulting in a 'tail' hodograph at the end of the simulation. Specifically, we define a tail hodograph as one that is curved at lower levels and straight at upper levels, as shown in Figure 4.

Prior studies involving tail hodographs in weakly-sheared environments have concluded that left-flank activity is generally enhanced due to storm-relative winds and convergence along the gust front, which aids new cell development. Straightline hodographs, on the other hand, produce mirror-image left- and right-flank storms with respect to the shear vector. When the hodograph changes from purely straightline to tail in a weak-shear regime, it is found that multicellular midlevel updrafts with straddling vortex couplets continue to be the favored mode and generally remain flank-unbiased. Hence, the incorporation of low-level curvature in this

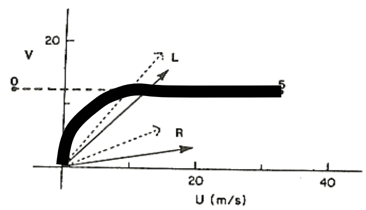

Figure 4: A tail hodograph (thickly drawn), defined as curved at lower levels and straight at upper levels (from Weisman and Klemp, 1986).

weak wind shear regime does not appear to significantly lead to the favoring of a particular flank as would be anticipated.

3.4 Strong Shear, Straightline-to-Tail Hodographs

Using the same straightline-to-tail change in hodograph shape over time, we increase overall shear magnitude to higher values (shear parameter Us=30 m s^{-1}) compared with the previous set of simulations. As the straightline control case produces mirror left- and right-flank supercells and the tail control case generates an enhanced, rotating, right-moving supercell, our experimental case results in the sustenance and eventual enhancement of a rotating, right-flank storm as well as possible organization of convection into bowed structures. Interestingly, this temporally-varying environment also transiently favors the left-flank storm in early simulation times. According to Bunkers (2002), left-moving supercells can exist in environments identified by shallow, low-level clockwise curvature, such as that present at early model times. Thus, as low-level curvature is added to the hodograph in a strongly-sheared environment, the storm system retains quasi-symmetric characteristics over extended periods before favoring the right-moving storm.

4. CONCLUSIONS

Temporal variations in environmental vertical shear are found to have a significant impact on simulated convective storms, at times resulting in systems that differ significantly from those one would predict using either the initial or final hodograph. For example, multicell storms in environments characterized by straightline hodographs appear to organize into bowed structures (rather than supercells) as the magnitude of the shear increases, while those evolving in environments with clockwise-curved hodographs eventually do produce right-flank supercells as the radius of the hodograph increases. In both instances, delaying the onset of the shear change until one hour after initiation makes a significant difference. For the curved hodograph case, this delay prevents the development of a right-flank supercell.. Adding low-level clockwise curvature in a weakly-sheared environment does not seem to produce a preference for either flank of the multicellular storm system. When low-level curvature is added in a strongly-sheared environment, the convective system remains quasi-symmetric for some time before favoring the right-flank storm. Initial slight enhancement of the left-flank storm as well as organized multicellular structures at later times are also noted in this case.

5. ACKNOWLEDGEMENTS

This research was supported by the National Science Foundation under Grant ATM99-81130. We thank Paul Markowski and John Clark for helpful comments on this research.

6. REFERENCES

Asselin, R., 1972: Frequency filter for time integrations. *Mon. Wea. Rev.*, **100**, 487-490.

Bunkers, M.J., 2002: Vertical wind shear associated with left-moving supercells. *Wea. Forecasting*, **17**, 845-855.

Kost, J.K., 2004: *Impacts of temporally variable environmental vertical wind shear upon numerically simulated convective storms.* M.S. Thesis, Department of Meteorology, Penn State University, 106 pp.

Moeng, C.H., and J.C. Wyngaard, 1988: Spectral analysis of large-eddy simulations of the convective boundary layer. *J. Atmos. Sci.*, **45**, 3573-3587.

Richardson, Y.P., and K.K. Droegemeier, 1996: An investigation of the dynamics governing organized multicell rotation and transition. Preprints, *18th Conf. on Severe Local Storms*, San Francisco, CA, Amer. Meteor. Soc., 195-199.

____, Y.P., 1999: *The influence of horizontal variations in vertical shear and low-level moisture on numerically simulated convective storms*. Ph.D. Dissertation, Department of Meteorology, University of Oklahoma-Norman, 236 pp.

Weisman, M.L., and J.B. Klemp, 1982: The dependence of numerically simulated convective storms on vertical wind shear and buoyancy. *Mon. Wea. Rev.*, **110**, 504-520.

_____, and _____, 1984: The structure and classification of numerically simulated convective storms in directionally varying wind shears. *Mon. Wea. Rev.*, **112**, 2479-2498.

_____, and _____, 1986: Characteristics of isolated convective storms. *Mesoscale Meteorology and Forecasting*, Peter S. Ray, Ed., American Meteorological Society, 331-358.

Xue, M., K.K. Droegemeier, V. Wong, A. Shapiro, and K. Brewster, 1995: *ARPS Version 4.0 User's Guide*, Center for Analysis and Prediction of Storms, University of Oklahoma, 381 pp.